Dislocation multiplication, exhaustion and mechanical behaviour for Ge single crystals

2002 J. Phys.: Condens. Matter 14 12989

(http://iopscience.iop.org/0953-8984/14/48/342)

INSTITUTE OF PHYSICS PUBLISHING JOURNAL OF PHYSICS: CONDENSED MATTER

J. Phys.: Condens. Matter **14** (2002) 12989–12995 PII: S0953-8984(02)54064-9

Dislocation multiplication, exhaustion and mechanical behaviour for Ge single crystals

Corinne Dupas, Nadia Zuodar, Olivier Coddet, Tomas Kruml and Jean-Luc Martin

IPMC, FSB, Ecole Polytechnique Fédérale de Lausanne, CH 1015 Lausanne, Switzerland

E-mail: jean-luc.martin@epfl.ch

Received 27 September 2002
Published 22 November 2002
Online at stacks.iop.org/JPhysCM/14/12989

Abstract

Dislocation multiplication and exhaustion processes in germanium are revisited in the light of new data from mechanical test transients. They are documented by transmission electron microscope (TEM) observations and dislocation velocity measurements by the etch pit technique. The transient tests consist of stress relaxations, creep tests and stress dip tests performed along the monotonic curve. The relaxation and creep curves exhibit a non-logarithmic dependence on time, unlike in other classes of materials. Dislocation multiplication is evidenced by these transient curves before the upper yield point. In addition, after the lower yield point, dislocation exhaustion takes place at the end of the transient. Some evidence of strain localization is also provided by strain dip tests and transmission electron micrographs.

(Some figures in this article are in colour only in the electronic version)

1. Introduction

A body of experimental data is available on the plasticity of diamond cubic covalent crystals and the associated microstructures [1, 2]. However, several points still deserve clarification such as the laws and processes associated with dislocation multiplication and the role of dislocation annihilation. Former data on the multiplication yield point in Ge have been reconsidered [3]. The authors conclude that two to three temperature domains have to be separated while the corresponding mechanisms need to be further investigated.

In addition, 3D computer simulations of dislocation sources have been performed recently for Si [4]. A new dislocation multiplication law was proposed which differs from the former empirical relation given by [1]. However, the geometry and densities of sources in the simulation are at variance with those observed in *in situ* x-ray topography experiments [5].

The present study addresses the above issues in characterizing several aspects of the deformation behaviour of Ge single crystals. This material is far less documented than Si. Preliminary work can be found in [6].

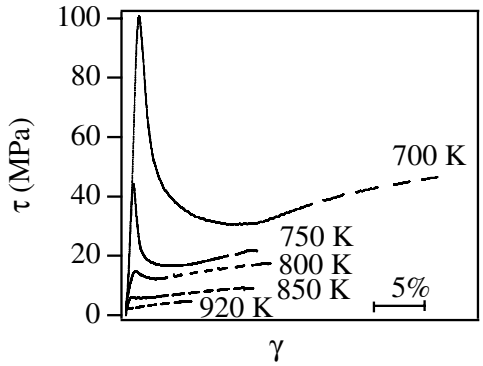

Figure 1. Stress–strain curves as a function of temperature. Transient tests are performed where the curves are interrupted.

2. Experiment

Intrinsic Ge single crystals were cut in ⟨123⟩ single-glide orientation with {111} and {154} lateral faces. Care was taken to remove the dislocation-rich surface layers. The compression specimens were deformed in a computer-controlled Schenck RMC 100 set-up, equipped with a furnace, under a flux of He. The temperature range was 700–900 K at a strain rate of 8.6×10^{-5} s^{-1}. Transient tests were performed along the stress–strain curve. These are commonly used in the field of metallic crystals. They consisted of stress relaxations, creep tests [7] and strain dip tests. The latter were performed as follows: at a given point of the deformation curve, the specimen is unloaded by an amount $\Delta\tau_1$, and allowed to creep. At the same point of the curve of a similar specimen, the unloading is $\Delta\tau_2 > \Delta\tau_1$ etc. A positive or negative creep rate can be observed corresponding respectively to small and large $\Delta\tau$ values. For intermediate ones, a zero creep rate sets in. The corresponding stress is considered as the internal stress. Such tests are usually performed during creep experiments [8], while at constant strain rate, a dedicated program has to be used for proper control of the machine.

Transmission electron microscope (TEM) foils were prepared by ion milling and observed in a CM 20 Philips microscope operating at 200 kV. The corresponding Ge samples were cooled under load so as to freeze the dislocation structures.

Etch pit experiments were used to measure dislocation velocities along the {145} face of the specimens. These were predeformed at 1000 K up to strains of 5×10^{-2} to create appropriate homogeneous dislocation populations. Subsequently, the specimen was subjected to a sudden stress increment $\Delta\tau$ for a duration Δt at a lower temperature. Etch pitting is performed prior to and after the stress increment to estimate the distance moved by the dislocation during Δt.

3. Mechanical test results

The stress–strain curves are shown in figure 1 as a function of temperature. The well known multiplication yield point disappears as the temperature increases, while the deformation mode shifts from heterogeneous to homogeneous.

Most transient tests were performed after the lower yield point (LYP) and a few ones before the upper yield point (UYP). For comparison, the same onset stress was chosen for a transient performed before the UYP and after the LYP on a given monotonic curve. A stress relaxation of 300 s duration is presented in figure 2. A remarkable feature is that subsequent

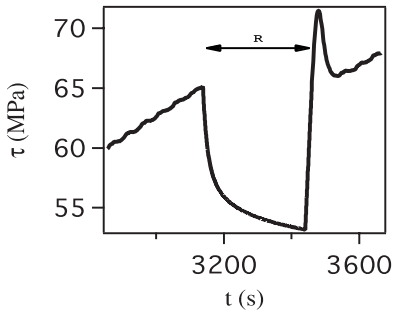

Figure 2. The stress relaxation test R during a monotonic test after the LYP. $T = 700$ K, $\tau = 65$ MPa, $\gamma_p = 24 \times 10^{-2}$.

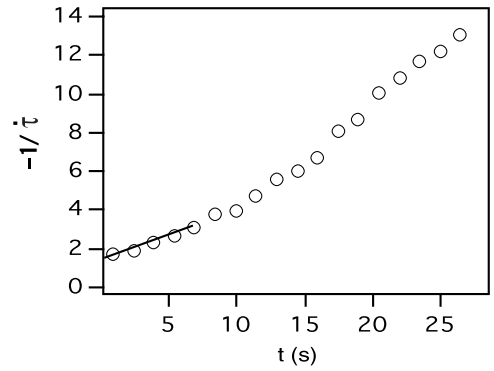

Figure 3. Reciprocal of the stress rate versus time. Stress relaxation at 700 K after the LYP, $\tau = 38$ MPa, $\gamma_p = 19 \times 10^{-2}$.

constant-strain-rate reloading induces a marked yield point. This is attributed to dislocation exhaustion during the transient. Consequently, a stress increment is needed to restore the same mobile dislocation density after the transient. This phenomenon is not observed, as a rule, in various classes of materials submitted to the same type of test [7]. Moreover, inspection of stress relaxation and creep curves shows that they do not follow a logarithmic variation in time. This is illustrated in figure 3 for a typical stress relaxation. The reciprocal of the stress rate plotted as a function of time is obviously non-linear, as it should be for a logarithmic relaxation [7]. However, a linear dependence is acceptable in figure 3 at the onset of the test, i.e. for $t < 10$ s. This yields an apparent activation volume V_a (proportional to the slope of the curve) of $48b^3$ in the present case, where b is the Burgers vector. The evolution of this volume as a function of time can be accounted for as follows. For such an experiment

$$V_a = kT(\partial \ln \dot{\gamma}_p / \partial \tau)$$

where $\dot{\gamma}_p$ is the plastic strain rate. It can be expressed using the well known Orowan relation [7]:

$$V_a = kT(\partial \ln \rho_m / \partial \tau + \partial \ln v / \partial \tau)$$

where v and ρ_m are respectively the average mobile dislocation velocity and density. As stress decreases (i.e. time increases), since v is a power function of stress (section 5), $\partial \ln v / \partial \tau$ increases. Since V_a increases in figure 3, it is not possible to reach a conclusion about the variation of ρ_m. However, some dislocation exhaustion takes place, as suggested by the reloading yield point.

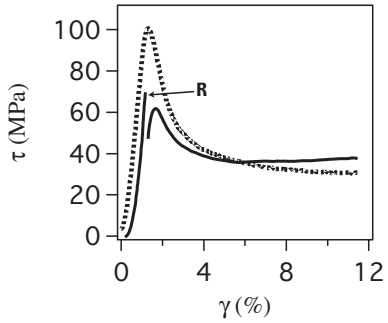

Figure 4. Stress–strain curves at 700 K. The dotted curve corresponds to a monotonic test, the full curve to a similar test with a stress relaxation R before the UYP starting at $\tau = 66$ MPa.

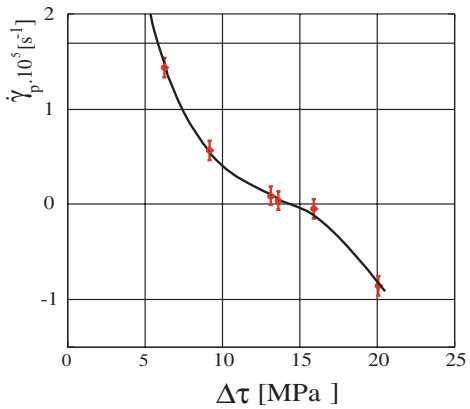

Figure 5. Stress dip tests at 750 K, $\tau = 33.8$ MPa, $\gamma_p = 18 \times 10^{-2}$. See the text.

An example of a relaxation test performed before the UYP is illustrated in figure 4. A monotonic curve, recorded under the same conditions, is shown for comparison. The relaxation curve exhibits an almost linear decrease of stress with time over 300 s. This evidences an almost constant stress rate (i.e. constant plastic strain rate [7]) as a function of time. It is thought that the lack of dislocations and the necessity for multiplication before the UYP are responsible for the peculiar shape of the curve. It is also remarkable that the amplitude of the yield point is considerably reduced after the relaxation R, as compared to the UYP of the monotonic curve. This confirms that abundant dislocation multiplication takes place during the transient.

The behaviour of the crystals under strain dip test conditions is illustrated in figure 5. Each data point corresponds to a different specimen. Figure 5 represents the creep rate $\dot{\gamma}_p$ immediately after unloading by an amount $\Delta\tau$. The zero creep rate corresponds here to $\Delta\tau = 14$ MPa, starting at 33.8 MPa, i.e. $\tau_i = 19.8$ MPa in the present case. Similar tests performed along the monotonic curve after the LYP allow the determination of τ_i as a function of strain (figure 6). $\tau_i(\gamma)$ is an increasing function since the dislocation density increases with the strain. The thermal part of the stress $(\tau - \tau_i)$ is approximately constant along the curve, since the lattice resistance to glide is constant too. This result complies with earlier estimations of τ_i using a different method [9]. A striking feature of figure 5 is that marked negative creep rates are observed for large $\Delta\tau$s. This is not observed in other types of crystal such as Cu in stage II and Ni_3Al [10] which are known to deform homogeneously. However, a similar

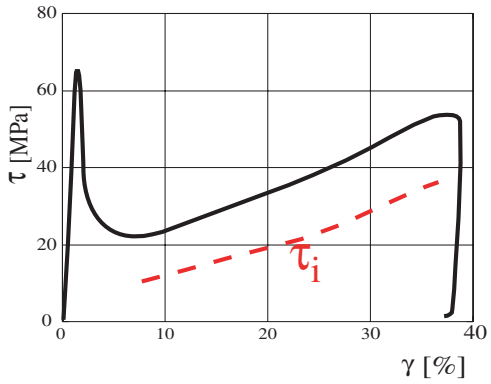

Figure 6. The athermal component of stress τ_i measured by strain dip tests, 750 K.

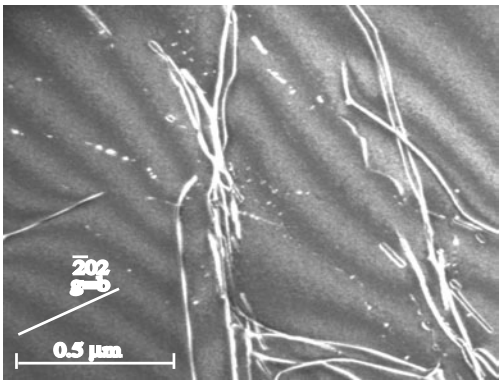

Figure 7. Dislocation structure after deformation at 750 K, $\tau = 25$ MPa. The foil is parallel to the primary glide plane.

effect is observed in Cu–7.5% Al [10] which deforms heterogeneously [11]. Therefore the negative creep rates in figure 5 are thought to be the signature of dislocation groups moving backwards for large stress reductions. This effect is difficult to detect in crystals deforming homogeneously.

4. TEM observations

Figure 7 illustrates dislocation structures after the LYP in a foil cut parallel to the primary slip plane. Dislocations are aligned along ⟨110⟩ directions (screws and 60° dislocations). Dipoles are perpendicular to the primary Burgers vector $b = (1/2)[\bar{1}01]$ (edges orientation). The dipoles are thought to form through interactions of dislocations with opposite Burgers vectors gliding along neighbouring parallel planes. Another interesting feature of figure 7 is the presence of numerous small dislocation loops that result from the dipole annealing, through short-distance climb for edges or cross-slip for screws. The two processes of dipole formation and annihilation contribute to the mobile dislocation exhaustion evidenced and the yield point at reloading after the transient tests in figure 2. The microstructural features exhibit some common points with previous observations for Si [12].

Figure 8 provides direct evidence of strain localization after the LYP in a foil cut perpendicular to the primary slip plane and containing the Burgers vector. Therefore the

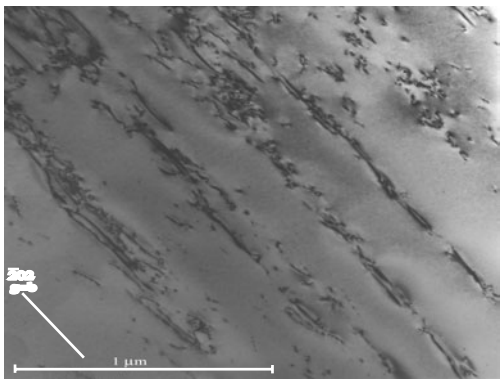

Figure 8. Dislocation structure after deformation at 750 K and $\tau = 34$ MPa. The foil plane is parallel to $1\bar{2}1$.

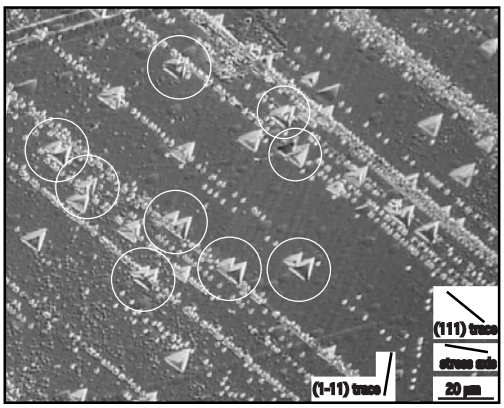

Figure 9. An example of a dynamic etch pit experiment performed at 750 K, for the {145} sample face. See the text.

long dislocations parallel to $[\bar{2}02]$ are in screw orientation. The active slip volume consists of layers of about 0.15 μm thickness, separated by undeformed zones about 0.3 μm thick. This observation supports the interpretation of the strain dip tests of figure 5.

5. Dislocation velocity measurements

Figure 9 shows typical etch pits after two successive load increments. During the first one, dislocations have moved over a short distance, so v can be determined, while during the second one, sources started operating along well defined planes. Velocity values are reported in figure 10 at 750 and 850 K respectively. They fit rather well to a power law dependence: $v = B(T)(\tau/\mu)^m$, μ being the shear modulus. The m-values are 2.1 ± 0.2 and 2.5 ± 0.3 at 750 and 850 K respectively. They agree fairly well with earlier measurements [13, 14]. These data allow us to compute activation energies Q of v through the relation $Q = kT^2(\partial \ln v/\partial T)_r$. The Q-values are close to 1.5 eV, which is the activation energy for screws measured by [14]. The present velocity values are used in a complementary study [15].

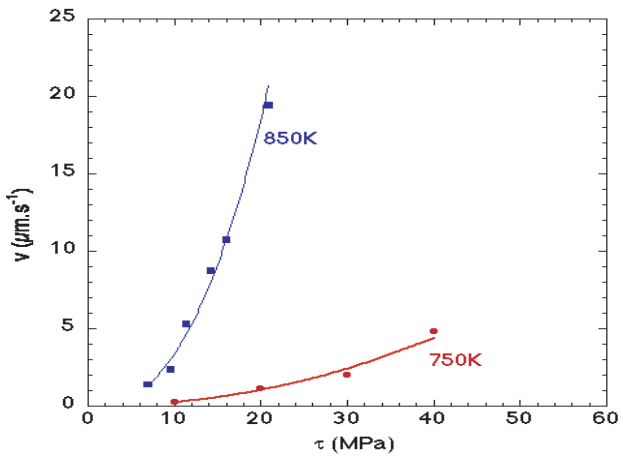

Figure 10. Dislocation velocity–stress relationships at two temperatures.

6. Discussion and conclusions

A new set of data related to macroscopic deformation tests (monotonic and transient ones) and microscopic observations (TEM and etch pit studies) emphasize the role of dislocation multiplication and exhaustion in the deformation mechanisms of Ge between 700 and 1000 K. Dislocation multiplication during transient tests before the UYP is extremely active. After the LYP, dislocation exhaustion is significant during the relaxation test. This latter process involves the annihilation of dipoles that form during straining. A multiplication yield point is present during reloading after the transient which compensates for dislocation exhaustion. After the LYP, hardening is due to the increase of dislocation density and corresponding internal stress. Some degree of glide heterogeneity is also observed under these conditions.

Acknowledgments

The financial support of Fonds National Suisse is gratefully acknowledged. CIME is thanked for providing the electron microscope facility.

References

[1] Alexander H and Haasen P 1968 *Solid State Phys.* **22** 28
[2] George A and Rabier J 1987 *Revue Phys. Appl.* **22** 941
[3] Siethoff H, Ahlborn K and Schröter W 1999 *Phys. Status Solidi* a **174** 205
[4] Moulin A, Condat M and Kubin L P 1999 *Acta Mater.* **47** 2879
[5] Vallino F, Jacques A and George A 2000 *Phys. Status Solidi* b **222** 51
[6] Charbonnier C, Kruml T and Martin J L 2001 *Multiscale Modeling of Materials (MRS Symp. Proc. vol 653c)* (Warrendale, PA: Materials Research Society) p Z 5.7.1
[7] Martin J L, Lo Piccolo B, Kruml T and Bonneville J 2001 *Mater. Sci. Eng.* A **322** 118
[8] Milicka K 1999 *Acta Mater.* **47** 1831
[9] Sumino K and Kojima K I 1971 *Cryst. Lattice Def.* **2** 159
[10] Coddet O and Kruml T 2002 at press
[11] Neuhäuser H and Schwink C 1993 *Material Science and Technology* vol 6 (Weinheim: VCH) p 191
[12] Allem R, Michel J P and George A 1989 *Phil. Mag.* A **52** 273
[13] Patel J R and Friedland P E 1971 *J. Appl. Phys.* **42** 3298
[14] Schaumburg H 1970 *Phys. Status Solidi* **40** K1
[15] Fikar J, Kruml T, Viguier B and Dupas C 2002 *J. Phys.: Condens. Matter* **14**